THE UNIVERSITY of EDINBURGH

Edinburgh Research Explorer

In-situ abiogenic methane synthesis from diamond and graphite under geologically relevant conditions

Citation for published version:
Pena Alvarez, M, Brovarone, AV, Donnelly, M-E, Wang, M, Dalladay-Simpson, P, Howie, R & Gregoryanz, E 2021, 'In-situ abiogenic methane synthesis from diamond and graphite under geologically relevant conditions', *Nature Communications*, vol. 12, 6387, pp. 1-5. https://doi.org/10.1038/s41467-021-26664-3

Digital Object Identifier (DOI):
10.1038/s41467-021-26664-3

Link:
Link to publication record in Edinburgh Research Explorer

Document Version:
Peer reviewed version

Published In:
Nature Communications

General rights
Copyright for the publications made accessible via the Edinburgh Research Explorer is retained by the author(s) and / or other copyright owners and it is a condition of accessing these publications that users recognise and abide by the legal requirements associated with these rights.

Take down policy
The University of Edinburgh has made every reasonable effort to ensure that Edinburgh Research Explorer content complies with UK legislation. If you believe that the public display of this file breaches copyright please contact openaccess@ed.ac.uk providing details, and we will remove access to the work immediately and investigate your claim.

OPEN ACCESS

Download date: 07. May. 2023

In-situ abiogenic methane synthesis from diamond and graphite under geologically relevant conditions

Miriam Peña-Alvarez[1], Alberto Vitale Brovarone[2,3], Mary-Ellen Donnelly[4], Mengnan Wang[1], Philip Dalladay-Simpson[4], Ross Howie[4], Eugene Gregoryanz[1,4,5]

[1]Centre for Science at Extreme Conditions and School of Physics and Astronomy, University of Edinburgh, Edinburgh, U.K.

[2]Dipartimento di Scienze Biologiche, Geologiche e Ambientali (BiGeA), Alma Mater Studiorum Università di Bologna, Piazza di Porta San Donato 1, 40126 Bologna, Italy

[3]Sorbonne Université, Musum National d'Histoire Naturelle, UMR CNRS 7590, IRD, Institut de Miná ralogie, de Physique des Matáriaux et de Cosmochimie, IMPMC, 75005 Paris, France

[4]Center for High Pressure Science and Technology Advanced Research (HPSTAR), Shanghai, China

[5] Key Laboratory of Materials Physics, Institute of Solid State Physics, Chinese Academy of Sciences, Hefei, China.

Abstract

The existence of deep, abiotic hydrocarbons in the upper mantle of the Earth, and their role in the deep subsurface biosphere together with oil and gas reservoirs, has long been a matter of scientific intrigue[1,2]. Diamond and graphite are fundamental sources of carbon in the upper mantle, and their reactivity with H_2-rich fluids present at these depths[3,4] may represent

the key to unravelling deep abiotic hydrocarbon formation. Here, we demonstrate an unexpected high reactivity between carbons' most common allotropes, diamond and graphite, with hydrogen at conditions comparable with those in the Earth's upper mantle along subduction zone thermal gradients[10]. Between 0.5-3 GPa and at temperatures as low as 300°C, carbon reacts readily with H_2 yielding methane (CH_4), whilst at higher temperatures (500°C and above), additional light hydrocarbons such as ethane (C_2H_6) emerge. These results suggest that the interaction between deep H_2-rich fluids and reduced carbon minerals may be an efficient mechanism for producing abiotic hydrocarbons at the upper mantle.

1 Introduction

The process of abiotic hydrocarbon formation in the deep Earth is still contested, despite being central in geo-biological processes and potential natural energy sources[1,2]. Light hydrocarbons of abiotic origin have been identified in an increasing number of geological fluids in the Earth's lithosphere[11–14]. Methane has also been detected within deep diamonds suggesting the presence of abiotic hydrocarbons at mantle depths[3,4,15]. However, their formation mechanisms and distribution, as well as their possibility to degas towards the crust and the atmosphere, remain largely unconstrained. The abiotic formation of stable light hydrocarbons, such as CH_4, was mainly considered to occur through reduction paths, and generally, in the presence of oxygen carrying species such as CO or CO_2 through the so-called Fischer-Tropsch Type (FTT) reactions[16–20].

In the Earth's interior, diamond and graphite are major carbon reservoirs,[20] while hydrogen is among the most volatile fluid elements. Graphite and other forms of carbonaceous materials are

dominant at depths between 50 and 140 km (2-4 GPa)[20–22], whilst deeper than 140 km depth (4 GPa) diamond becomes stable[23]. In Fig. 1 we summarise the relationship between pressure, in deep in the Earth's mantle, and the evolution of the distribution of graphite and diamond, together with hydrogen and methane clusters.

Methane may be a fundamental component of upper mantle fluids [20]. It reacts under high pressure, forming long-chain hydrocarbons and then it is predicted to eventually dissociate into diamond, graphitic carbon and hydrogen[5,6,9,24]. Methane at depths could co-exist with molecular hydrogen (H_2)and small amounts of light hydrocarbons and different carbon allotropes[16,19,20]. However, the origin of methane in the upper mantle remains largely unconstrained [2].

Reactions between H_2-rich fluids and carbon-bearing parent minerals may be effective to produce methane and other hydrocarbons abiotically. At upper mantle conditions, H_2 may be present and immiscible in aqueous fluids and react with condensed carbon minerals[25–29]. Water-rock interactions at subduction zone conditions may also be effective in generating H_2-rich fluids [14,30–34], also in the presence of graphite [28,35,36]. Molecular hydrogen may also be present in minerals at upper mantle conditions [37]. Recent analysis of fluid inclusions in super-deep diamonds indicates that H_2 may represent a significant component of upper mantle fluids in the presence of diamond[3,4]. Yet, reactivity between diamond and H_2 at upper mantle conditions has not been contemplated as a source of abiogenic hydrocarbons.

Here, we investigate abiotic methane production from the precursors of pure H_2 and condensed carbon minerals such as diamond and graphite. We conduct *in-situ* experiments using a

resistively heated diamond anvil cell (DAC) at pressure and temperature conditions in the range of 0.5 to 5 GPa and 300 to 730°C, and use Raman spectroscopy as the diagnostic tool. Most of the investigated conditions are consistent with Earth's upper mantle and subduction zone *P-T* gradients[10]. We find that at these mild *P-T* conditions, diamond and graphite react readily with H_2 to form methane and other light hydrocarbons, such as ethane (C_2H_6). This demonstrates that the reaction between condensed carbon phases and H_2, could be an important source of abiotic hydrocarbons, that should be considered in the deep Earth's carbon cycle.

2 Results

Diamond and hydrogen. At room temperature and at pressures between 2-3 GPa, Raman measurements show only the characteristic spectrum of the H_2 sample, and that of the diamond anvils (Fig. 2). Heating hydrogen in a DAC at 2 GPa (which corresponds to Earth depths of about 70 km,[38] see Fig. 1) to temperatures of 500°C, we observe a new Raman band appearing at $\sim$2900 cm^{-1} within approximately twenty minutes (see Fig. 2). This new band can be detected uniformly across the sample chamber. Repeating measurements at 3 GPa (below or around 70 km depth, see Fig. 1), and holding the sample at lower temperatures of 300°C for a period of two hours, the same results are observed, a new band at 2900 cm^{-1} appears and its intensity grows with time. This new mode coincides with the most intense C-H vibrational stretching mode of methane, indicating abiotic methane production from the only elements present in the experimental chamber: hydrogen and diamond.

High temperature studies of dense methane have yielded other light hydrocarbons such as ethane (C_2H_6), propane (C_3H_8), butane (C_4H_{10}) and isobutane (C_4H_{10})[6]. In our experiments, increasing temperature to 730°C at 3 GPa, leads to the growth of more complex vibrational excitations, centred around $\sim$2950 cm^{-1}, Fig. 2b. The intensity of these modes increases with time if the sample is held at above 500°C for 2 hours. By comparing the obtained spectrum with spectra reported for hydrocarbons in the literature[39–41], we can identify the additional product as ethane (C_2H_6). Upon temperature quenching, samples were subsequently compressed up to 30 GPa at room temperature. The evolution of the vibrational spectra and their frequencies versus pressure are in good agreement with those of methane and ethane (Supplementary Fig. 2)[39,42,43]. We also note that at above 5 GPa we observe an additional vibrational mode, which is present neither in pure methane nor in hydrogen (see mode indicated by asterisks in Fig. 2a). This new mode has previously been interpreted as being a feature of a CH_4-H_2 van der Waals compounds[43]. Experiments were repeated using deuterium as a precursor instead of hydrogen, in which we observed the formation of CD_4, Supplementary Fig. 1. The presence of CD_4 after heating is evidence that the reaction is between the D_2 sample and diamond, and not from residuals and/or a contaminant from the preparation process.

We have performed three control experiments to eliminate the possibility of carbon contaminants in the sample chamber, whereby the gasket and diamonds were insulated from the hydrogen sample with aluminium oxide (Al_2O_3), see Fig. 3. Al_2O_3 has been shown to form a protective layer that slows down hydrogen diffusion into diamond at high pressures and temperatures[44]. Therefore, it could preclude the formation of CH_4 from the diamond anvil and hydrogen. Inspection of the

optical images of the sample chamber after 1 hour at 360°C and 4 GPa reveals that the coating was still pristine (Fig. 3b) and no methane was observed spectroscopically. However, after 3 hours at this temperature, part of the coating began breaking up and detaching from the diamond, Fig. 3. This deterioration of the coating with temperature and time enabled hydrogen to reach the diamonds, forming methane on contact. We have also considered that the transition metals from which the gaskets are made, could catalyse the reactions[45]. We have conducted several heating runs with different gasket materials such as rhenium (Re), and tungsten (W); and gasket liners e.g. gold (Au) and Al_2O_3 (see Supplementary Table 1 for a list of the materials used). We observed that, regardless of the gasket and gasket insert materials, if the diamonds are not protected by Al_2O_3, CH_4 and/or C_2H_6 are always produced.

Graphite - glass-like carbon and hydrogen. Since graphite may be an important component of subducted sedimentary rocks[46–48] we have repeated our experiments by adding graphite into the sample chamber. These experimental runs yielded identical results producing larger amounts of methane on a shorter timescale than with the diamond precursor. We have also explored the reactivity of disordered carbonaceous materials using a glass-like form of carbon (for which thermodynamic data are available[48]), which may be common below 500-600°C in subduction zones[21]. Fig. 4 shows the Raman spectra between 1.0 and 1.5 GPa during heating cycles of (a) H_2-graphite and (b) H_2-glassy-like carbon. In both cases there is a rapid growth of the C-H stretching mode of methane with time. Similar to the methane production from diamond, CH_4 forms compounds with H_2 on compression of the quenched sample[43].

3 Discussion

In each of the graphite and glassy carbon experiments similar amounts of samples were used. Comparing the intensities of methane produced by different carbonaceous samples, one can conclude that glassy-like carbon and graphite are naturally more reactive to H_2 than diamond (see Supplementary Figure 4 to compare the relative intensities of methane peaks generated from the different starting materials). Of course, this statement is tentative and approximate, as the graphite and glassy-like carbon measurements also contain a contribution from the methane formed from the diamond anvils and there are other factors such as background and hydrogen accessibility to the carbonaceous sample that influence the experiment. Nevertheless, this suggests that graphitic carbon materials can act as an efficient reactant for abiotic CH_4 formation in upper mantle and crustal environments.

Condensed carbon reservoirs and their mobilisation in deep fluids may represent a key to unravelling deep carbon recycling. We have shown that under dry conditions, and in the absence of oxygen or a catalyst, methane is formed from diamond, graphite or glassy carbon and hydrogen, at conditions comparable to the outer layers of the Earth's mantle (depths of 18-160 km-pressures of 0.5 to 5 GPa and temperatures between 300 - 730°C). Fluids rich in H_2 may be common in the upper mantle and generated by fluid-rock or melt-rock reactions [14,14,49], or dissolved in minerals[37]. Moreover, immiscibility of H_2 or H_2-CH_4 in aqueous fluids in the graphite or diamond stability field[25–28] could extend the effectiveness of our results to local fluid-mineral interactions in oxygen-bearing systems. Fig. 1 summarises the main results of this work, in which we propose

that hydrogen and different reduced carbon species found in the Earth's mantle could be an important source of abiogenic hydrocarbons. Our results provide a possible explanation for geological findings of the detection of methane and hydrogen in diamonds extracted from the lower mantle[3,4]. Thus, the different species might contribute to the cycling of deep carbon in the Earth's upper mantle via methane production and act as sources of deep energy for shallower reservoirs[1,14,50].

4 Methods

Ultra-low fluorescent diamond anvils, with culet diameters ranging between 200-300 μm were used. Re-foil or W-foil gaskets were used to contain the samples. No differences were found when using Re or W or Au-lined Re gaskets. Research grade (99.9999 %) hydrogen and deuterium samples were gas loaded into diamond anvil cells (DACs) at a pressure of 0.2 GPa. Prior to gas loading, the diamond surfaces were thoroughly cleaned with several washes, first with acetone and then with of doubly distilled de-ionized water and the use of organic solvents was avoided. The gasket was first cleaned in water in an ultrasonic bath, and then placed on the diamond surface for immediate loading. After loading, samples were mapped with Raman spectroscopy to rule out any possible contamination. High-purity graphite (99.8 % , 43078 Alfa Aesar) and glass-like spherical powder by Alpha Aesar, were loaded into the DAC, and research grade hydrogen (99.9999%) was subsequently gas loaded at a pressure of 0.2 GPa. Al_2O_3 coatings were done via Chemical Vapour Deposition. High-quality Raman spectra were acquired using a custom-built micro-focused Raman system, using a 514 nm laser as the excitation line.

High-temperature experiments were conducted using modified high-temperature Mao-Bell diamond anvil cells equipped with a primary and a secondary heater and a thermocouples. A type-K thermocouple was partially clamped between the gasket and the diamond anvil. Good mechanical contact ensures a more accurate temperature measurement whilst ensuring optimum proximity to the sample chamber. Heating was done in two stages; the primary, external to the cell assembly heating to 500°C; a secondary internal heater, situated around the diamond anvils,

heating to 730°C. The secondary heater consisted of a Mo-coil heating element driven by a DC power supply on a feedback loop with a high sampling rate PID controller [51,52,54].

5 Data availability

The data that support the findings of this study are available from the corresponding author upon request.

6 References

1. Gold, T. The deep, hot biosphere. *Proc. Natl. Acad. Sci. U. S. A* **89**, 6045–6049 (1992).

2. Sephton, M. A. & Hazen, R. M. On the origins of deep hydrocarbons. *Rev. Mineral. Geochem.* **75**, 449–465 (2013).

3. Smith, E. M. *et al.* Large gem diamonds from metallic liquid in Earth's deep mantle. *Science* **354**, 1403–1405 (2016).

4. Smith, E. M. *et al.* Blue boron-bearing diamonds from Earth's lower mantle. *Nature* **560**, 84–87 (2018).

5. Benedetti, L. R. *et al.* Dissociation of CH_4 at high pressures and temperatures: diamond formation in Giant planet interiors? *Science* **286**, 100 – 102 (1999).

6. Kolesnikov, A., Kutcherov, V. G. & Goncharov, A. F. Methane-derived hydrocarbons produced under upper-mantle conditions. *Nat. Geosci.* **2**, 566 (2009).

7. Zerr, A., Serghiou, G., Boehler, R. & Ross, M. Decomposition of alkanes at high pressures and temperatures. *High Pres. Res.* **26**, 23–32 (2006).

8. Lobanov, S. S. *et al.* Carbon precipitation from heavy hydrocarbon fluid in deep planetary interiors. *Nat. Commun.* **4**, 1–8 (2013).

9. Hirai, H., Konagai, K., Kawamura, T., Yamamoto, Y. & Yagi, T. Polymerization and diamond formation from melting methane and their implications in ice layer of Giant planets. *Phys.*

Earth Planet. Inter. **174**, 242 – 246 (2009). Advances in high pressure mineral physics: from deep mantle to the core.

10. Penniston-Dorland, S. C., Kohn, M. J. & Manning, C. E. The global range of subduction zone thermal structures from exhumed blueschists and eclogites: rocks are hotter than models. *Earth Planet. Sci. Lett.* **428**, 243–254 (2015).

11. Charlou, J., Donval, J., Fouquet, Y., Jean-Baptiste, P. & Holm, N. Geochemistry of high h_2 and ch_4 vent fluids issuing from ultramafic rocks at the rainbow hydrothermal field. *Chem. Geo.* **191**, 345–359 (2002).

12. Etiope, G. & Sherwood Lollar, B. Abiotic methane on earth. *Rev. Geophys.* **51**, 276–299 (2013).

13. Young, E. *et al.* The relative abundances of resolved $^{l2}CH_2D_2$ and $^{13}CH_3D$ and mechanisms controlling isotopic bond ordering in abiotic and biotic methane gases. *Geochim. Cosmochim. Acta.* **203**, 235–264 (2017).

14. Vitale-Brovarone, A. *et al.* Subduction hides high-pressure sources of energy that may feed the deep subsurface biosphere. *Nat. Commun.* **11**, 1–11 (2020).

15. Smit, K. V., Shirey, S. B., Stern, R. A., Steele, A. & Wang, W. Diamond growth from C–H–N–O recycled fluids in the lithosphere: Evidence from CH_4 micro-inclusions and $\delta\ ^{13}$C–$\delta\ ^{15}$N–N content in marange mixed-habit diamonds. *Lithos* **265**, 68–81 (2016).

16. Anderson, R. B., Kölbel, H. & Ralek, M. *The Fischer-Tropsch synthesis*, vol. 16 (Academic Press New York, 1984).

17. McCollom, T. M. Laboratory simulations of abiotic hydrocarbon formation in Earth's deep subsurface. *Rev. Mineral. Geochem.* **75**, 467–494 (2013).

18. McCollom, T. M. Abiotic methane formation during experimental serpentinization of olivine. *Proc. Natl. Acad. Sci. U. S. A* **113**, 13965–13970 (2016).

19. Spanu, L., Donadio, D., Hohl, D., Schwegler, E. & Galli, G. Stability of hydrocarbons at deep earth pressures and temperatures. *Proc. Natl. Acad. Sci. U. S. A* **108**, 6843–6846 (2011).

20. Frost, D. J. & McCammon, C. A. The redox state of Earth's mantle. *Annu. Rev. Earth Planet. Sci.* **36**, 389–420 (2008).

21. Buseck, P. R. & Huang, B.-J. Conversion of carbonaceous material to graphite during metamorphism. *Geochim. Cosmochim. Acta* **49**, 2003–2016 (1985).

22. Zhang, C. & Duan, Z. A model for C–O–H fluid in the Earth's mantle. *Geochim. Cosmochim. Acta.* **73**, 2089–2102 (2009).

23. Day, H. W. A revised diamond-graphite transition curve. *Am. Min.* **97**, 52–62 (2012).

24. Hazen, R., Mao, H., Finger, L. & Bell, P. Structure and compression of crystalline methane at high pressure and room temperature. *Appl. Phys. Lett.* **37**, 288–289 (1980).

25. Bali, E., Audétat, A. & Keppler, H. Water and hydrogen are immiscible in earth's mantle. *Nature* **495**, 220–222 (2013).

26. Huang, F., Daniel, I., Cardon, H., Montagnac, G. & Sverjensky, D. A. Immiscible hydrocarbon fluids in the deep carbon cycle. *Nat. Commun.* **8**, 1–8 (2017).

27. Li, Y. Immiscible CHO fluids formed at subduction zone conditions. *Geochem. Perspect. Lett* **3**, 12–21 (2017).

28. Vitale-Brovarone, A. *et al.* Massive production of abiotic methane during subduction evidenced in metamorphosed ophicarbonates from the italian Alps. *Nat. Commun.* **8**, 1–13 (2017).

29. Griffin, W. L. *et al.* Super-reducing conditions in ancient and modern volcanic systems: sources and behaviour of carbon-rich fluids in the lithospheric mantle. *Mineralogy and Petrology* **112**, 101–114 (2018).

30. Ferrando, S., Frezzotti, M. L., Orione, P., Conte, R. C. & Compagnoni, R. Late-alpine rodingitization in the bellecombe meta-ophiolites (aosta valley, italian western Alps): evidence from mineral assemblages and serpentinization-derived H_2-bearing brine. *Int. Geol. Rev.* **52**, 1220–1243 (2010).

31. Boutier, A., Vitale-Brovarone, A., Martinez, I., Sissmann, O. & Mana, S. High-pressure serpentinization and abiotic methane formation in metaperidotite from the appalachian subduction, northern vermont. *Lithos* **396**, 106190 (2021).

32. Peng, W., Zhang, L., Tumiati, S., Vitale-Brovarone, A.,Hu, H., Cai, Y.& Shen, T. Abiotic methane generation through reduction of serpentinite-hosted dolomite: implications for carbon mobility in subduction zones. *Geochim. Cosmochim. Acta* **311**, 119–140 (2021).

33. Mao, H. K., Hu, Q., Yang, L., Liu, J., Kim, D. Y., Meng, Y., Zhang, L., Prakapenka, V., Yang, W., Mao, W. L. . *Natl. Sci. Rev.* **4**, 870–878 (2017).

34. Mao, H.-K., Mao, W. L., Key problems of the four-dimensional Earth system, *Matter Radiat. Extrem.* **5**, 038102 (2020).

35. Malvoisin, B., Chopin, C., Brunet, F. & Galvez, M. E. Low-temperature wollastonite formed by carbonate reduction: a marker of serpentinite redox conditions. *J. Petrol.* **53**, 159–176 (2012).

36. Galvez, M. E. *et al.* Graphite formation by carbonate reduction during subduction. *Nat. Geosci.* **6**, 473–477 (2013).

37. Moine, B. *et al.* Molecular hydrogen in minerals as a clue to interpret ∂D variations in the mantle. *Nat. Commun.* **11**, 1–10 (2020).

38. Dziewonski, A. M. & Anderson, D. L. Preliminary reference earth model. *Phys. Earth Planet. Inter.* **25**, 297–356 (1981).

39. Shimizu, H., Shimazaki, I. & Sasaki, S. High-pressure Raman study of liquid and molecular crystal ethane up to 8 GPa. *Jpn. J. Appl. Phys.* **28**, 1632 (1989).

40. Kudryavtsev, D. *et al.* Raman and IR spectroscopy studies on propane at pressures of up to 40 GPa. *J. Phys. Chem. A* **121**, 6004–6011 (2017).

41. Kudryavtsev, D. A., Kutcherov, V. G. & Dubrovinsky, L. S. Raman high-pressure study of butane isomers up to 40 GPa. *AIP Adv.* **8**, 115104 (2018).

42. Wu, Y., Sasaki, S. & Shimizu, H. High-pressure Raman study of dense methane: CH_4 and CD_4. *J. Raman Spectrosc.* **26**, 963–967 (1995).

43. Somayazulu, M. S., Finger, L. W., Hemley, R. J. & Mao, H. K. High-pressure compounds in methane-hydrogen mixtures. *Science* **271**, 1400 – 1402 (1996).

44. Subramanian, N., Goncharov, A. F., Struzhkin, V. V., Somayazulu, M. & Hemley, R. J. Bonding changes in hot fluid hydrogen at megabar pressures. *Proc. Natl. Acad. Sci. U. S. A* **108**, 6014–6019 (2011).

45. Chou, I.-M. & Anderson, A. J. Diamond dissolution and the production of methane and other carbon-bearing species in hydrothermal diamond-anvil cells. *Geochim. Cosmochim. Acta.* **73**, 6360–6366 (2009).

46. Beyssac, O., Goffé, B., Chopin, C. & Rouzaud, J. Raman spectra of carbonaceous material in metasediments: a new geothermometer. *J. Metamorph. Geol.* **20**, 859–871 (2002).

47. Hayes, J. M. & Waldbauer, J. R. The carbon cycle and associated redox processes through time. *Philos. Trans. R. Soc. Lond., B, Biol. Sci.* **361**, 931–950 (2006).

48. Tumiati, S. *et al.* Dissolution susceptibility of glass-like carbon versus crystalline graphite in high-pressure aqueous fluids and implications for the behavior of organic matter in subduction zones. *Geochim. Cosmochim. Acta.* **273**, 383–402 (2020).

49. Tollan, P., Gurenko, A. & Hermann, J. Elucidating the processes affecting highly primitive lavas of the borgarhraun flow (northern iceland) using trace elements in olivine. *Geochim. Cosmochim. Acta* **286**, 441–460 (2020).

50. Mukhina, E., Kolesnikov, A. & Kutcherov, V. The lower *PT* limit of deep hydrocarbon synthesis by $CaCO_3$ aqueous reduction. *Sci. Rep.* **7**, 1–5 (2017).

51. Gregoryanz, E., Goncharov, A. F., Matsuishi, K., Mao, H. K. & Hemley, R. J. Raman spectroscopy of hot dense hydrogen. *Phys. Rev. Lett.* **90**, 4 (2003).

52. Howie, R. T., Dalladay-Simpson, P. & Gregoryanz, E. Raman spectroscopy of hot hydrogen above 200 GPa. *Nat. Mater.* **14**, 495–499 (2015).

53. Li, J., Redfern, S.A.T., Giovannelli, D. Introduction: Deep carbon cycle though five reactions. *American Mineralogist* **104**, 465–467 (2019).

54. Peña-Alvarez, M. *et al.* Intensity of Raman modes as a temperature gauge in fluid hydrogen and deuterium. *J. Appl. Phys.* **125**, 025901 (2019).

7 Acknowledgements

M.P.A. acknowledges the support of the UKRI Future leaders fellowship Mrc-Mr/T043733/1. M.P.A. and E.G. acknowledge the support of the European Research Council (ERC) Grant "Hecate" Ref. No. 695527 held by Prof. Graeme Ackland. A.V.-B. was supported by an ERC CoG "DeepSeep" (No. 864045), an ANR T-ERC grant (No. LS171301), a MIUR Levi Montalcini grant, by the Deep Carbon Observatory (DCO) Deep Energy community, and by the Richard Lounsbery foundation. Josh Wood is thanked for technical support on Figure 1. R.T.H. acknowledges the support of the National Science Foundation of China (Grant No. 11974034) and ERC Grant "MetElOne" Reference No. 948895.

8 Author contributions

M.P.A, A.V.-B and E. G. planned the research. P.D.-S., E.G., and R.T.H. contributed materials/diagnostic tools. M.P.A., M.-E.D., M.W., P.D.-S., R.T.H. carried out the experiments. M.P.A analysed and interpreted the data. M.P.A, A. V.-B and E. G. wrote the paper.

9 Competing interests:

The authors declare no competing interests.

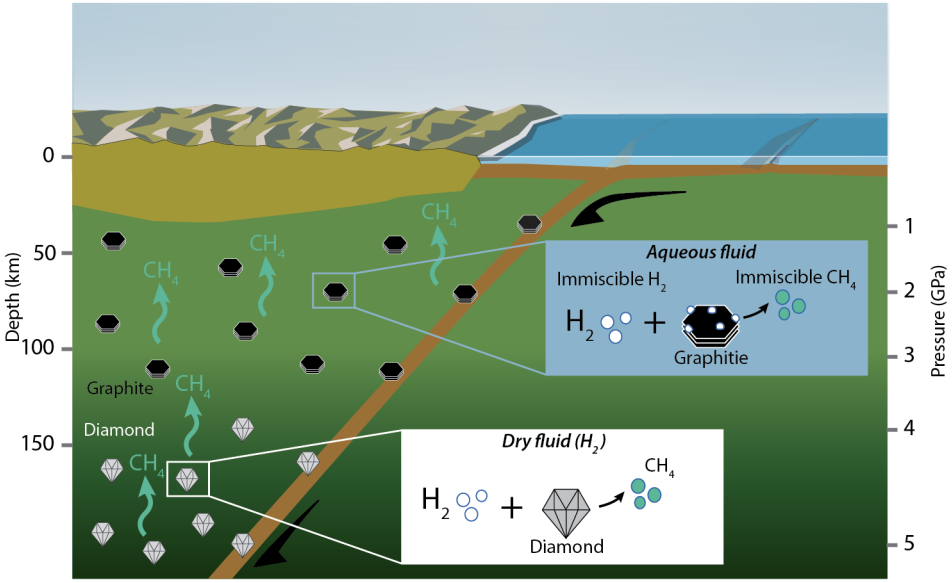

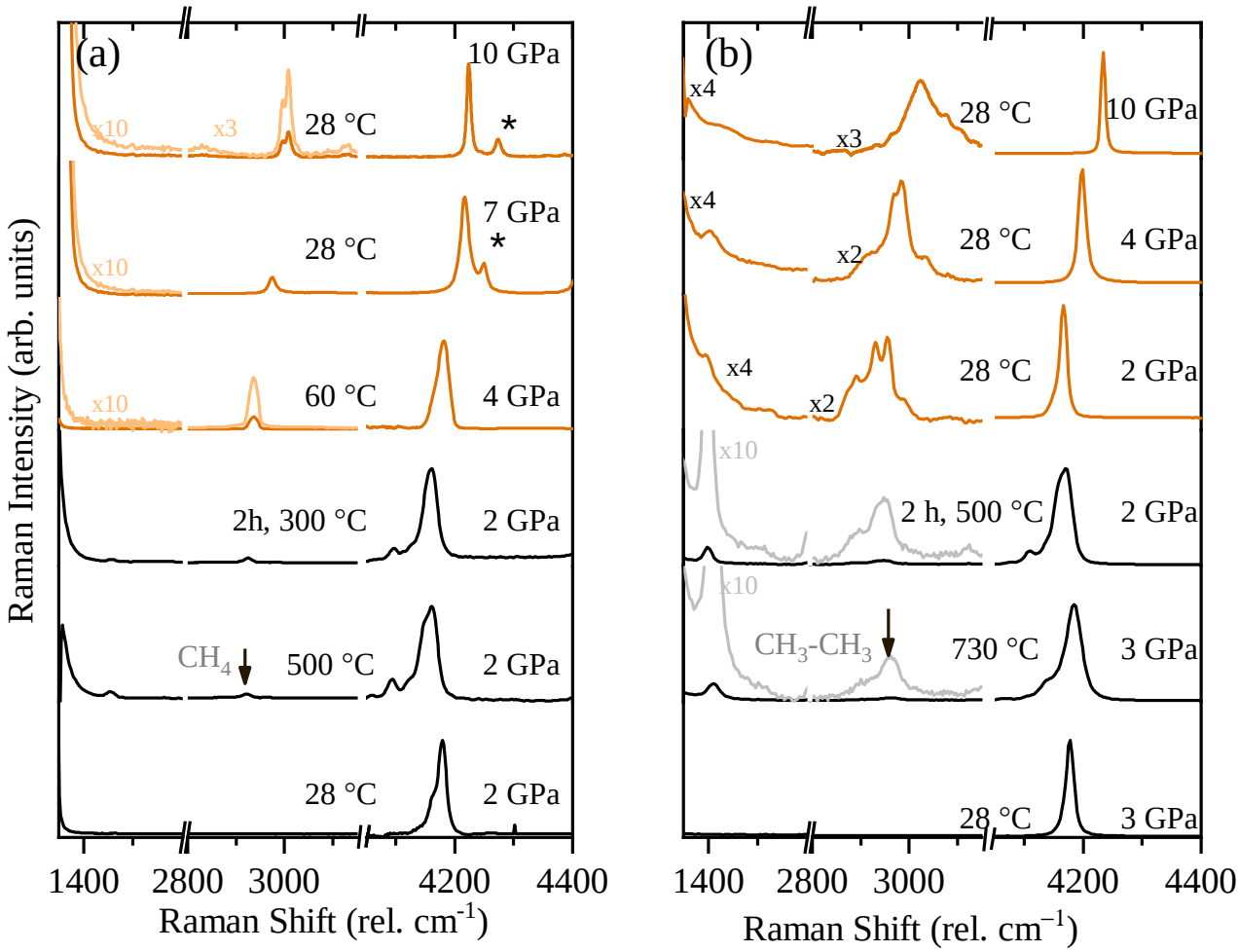
(a)
10 GPa
x10
x3
28 °C
*
7 GPa
28 °C
*
x10
x10
60 °C
4 GPa
2h, 300 °C
2 GPa
CH4
500 °C
2 GPa
28 °C
2 GPa
1400
2800
3000
4200
4400
Raman Intensity (arb. units)
Raman Shift (rel. cm-1)
(b)
x4
x3
28 °C
10 GPa
x4
x2
28 °C
4 GPa
x4
x2
28 °C
2 GPa
x10
2 h, 500 °C
2 GPa
x10
CH3-CH3
730 °C
3 GPa
28 °C
3 GPa
1400
2800
3000
4200
4400
Raman Shift (rel. cm−1)

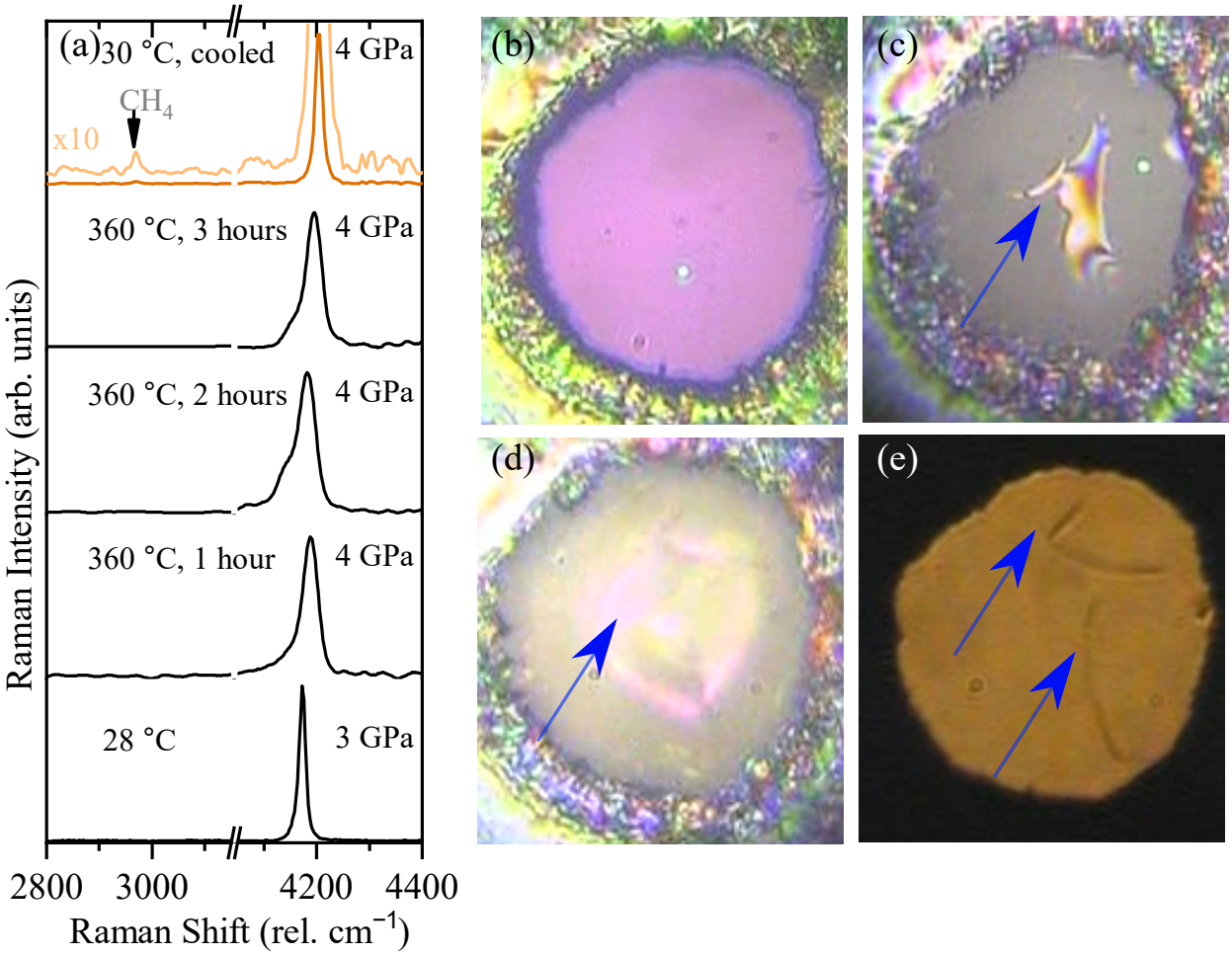
(a)
30 °C, cooled
4 GPa
CH4
x10
360 °C, 3 hours
4 GPa
360 °C, 2 hours
4 GPa
360 °C, 1 hour
4 GPa
28 °C
3 GPa
Raman Intensity (arb. units)
2800
3000
4200
4400
Raman Shift (rel. cm−1)
(b)
(c)
(d)
(e)

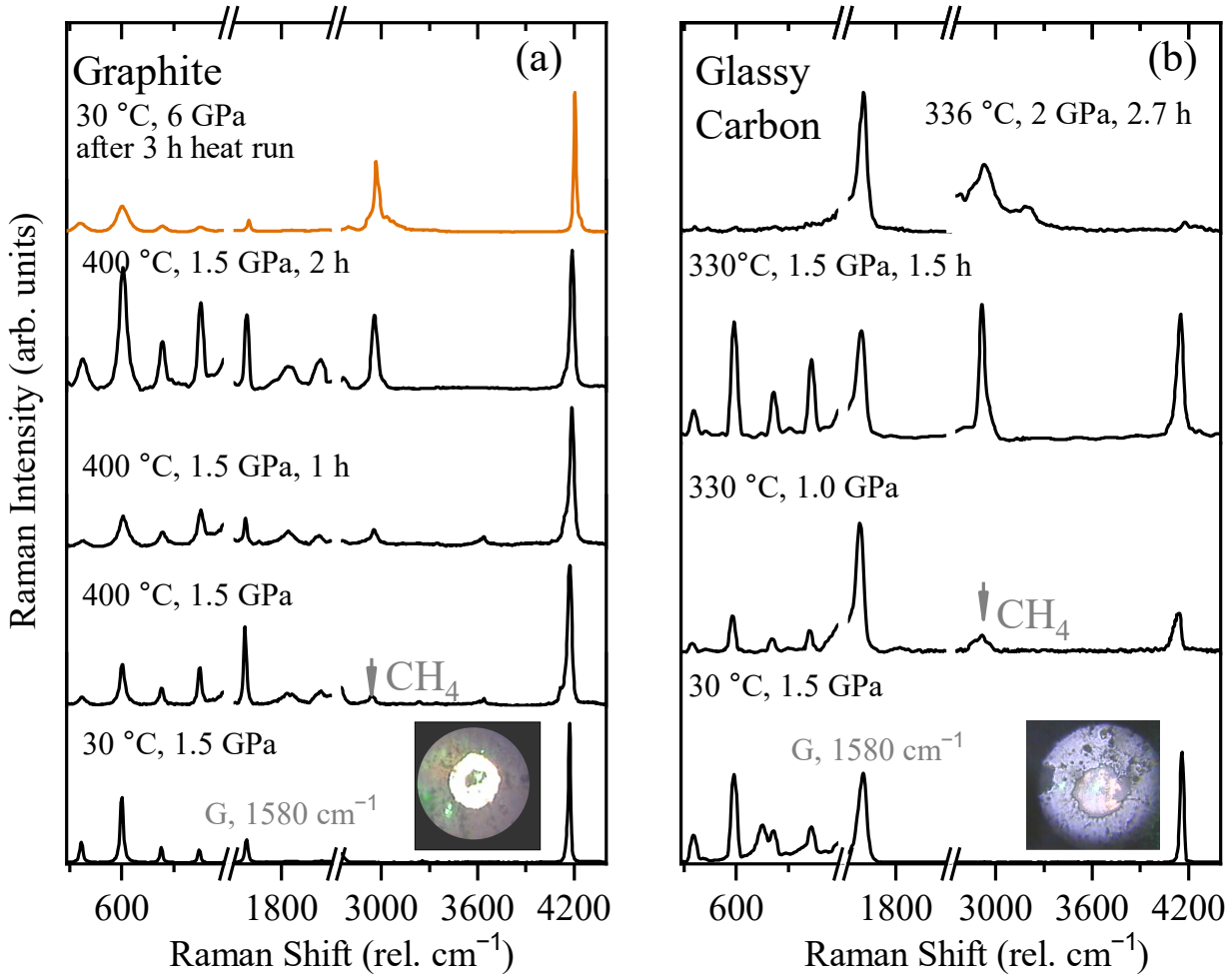
Graphite
(a)
30 °C, 6 GPa
after 3 h heat run
400 °C, 1.5 GPa, 2 h
400 °C, 1.5 GPa, 1 h
400 °C, 1.5 GPa
CH4
30 °C, 1.5 GPa
G, 1580 cm−1
Raman Intensity (arb. units)
600
1800
3000
3600
4200
Raman Shift (rel. cm−1)
Glassy
Carbon
(b)
336 °C, 2 GPa, 2.7 h
330°C, 1.5 GPa, 1.5 h
330 °C, 1.0 GPa
CH4
30 °C, 1.5 GPa
G, 1580 cm−1
600
1800
3000
3600
4200
Raman Shift (rel. cm−1)

Figure 1 Sketch modified after Figure 1 in Li *et al.*[53] summarising the implications of this study on the genesis of abiotic CH_4 in the upper mantle. Below about 140 km depth (4 GPa), the immiscibility of H_2 in aqueous fluids[25] can promote interactions between H_2 gas and graphitic carbon, leading to the formation of CH_4 (Fig. 3). This condition is plausible in reducing settings with low oxygen concentrations within the upper mantle[23] or where reducing conditions are generated in subduction zones[28]. At greater depths in the diamond stability field, the oxygen fugacity is predicted to be lower[20], and dry H_2 fluids are more common[3,4] and interact with diamond to form abiotic CH_4 (Fig. 1).

Figure 2 Raman spectra of resistive heating of hydrogen in a diamond anvil cell at selected pressures and temperatures. a) Up to a maximum temperature of 500°C and held at 300°C for two hours and after cooling down. Orange spectra correspond to the cooled down sample. b) Up to a maximum temperature of 730°C and held at 500°C for two hours and after cooling down. Orange spectra correspond to cooled down sample. The CH stretching modes of CH_4 (a) and C_2H_6 (b) appear between 2900 and 3000 cm^{-1}. In the cooled down sample of experiment b the CH wagging mode is seen at around 1480 cm^{-1}. The band at around 4200 cm^{-1} corresponds to the vibrational mode of H_2 (Q_1[52], this is accompanied by the rotational + vibrational band ($Q_1 + S_0$) visible in liquid hydrogen. At high temperatures there is another band at lower frequency which corresponds to the thermally populated second vibrational state of hydrogen[54]. Asterisks mark the vibrational mode from the CH_4-H_2 van der Waals compounds[43].

Figure 3 Hydrogen sample resistively heated during heating and cooling process at 3 GPa, using a diamond anvil cell whose culets and gasket hole had been coated with 300 μm Al_2O_3 with chemically vapour deposition. a) Representative Raman spectra during heating and cooling (orange spectrum). b) Image taken in transmitted and reflected light while being heated at 360 °C for 1 hour; c) Image of the sample at 360 °C for 3 hours, the image has been taken in reflected light so the region of the chamber where coating is becoming damaged is seen. d) Image of the sample after cooling in transmitted light. e) Image of the sample after cooling down only in transmitted light. Blue arrows are used to point the regions of the damaged Al_2O_3 layer; green spots are due to the laser beam.

Figure 4 Resistive heating of hydrogen in a diamond anvil cell. a) Graphite loaded together with H_2, spectra at selected temperatures and pressure. Spectra have been normalised to the H_2 stretching mode, around 4200 cm^{-1}. Orange spectrum correspond to the quenched sample. b) Glassy-like carbon loaded together with H_2, spectra are normalised to the G band characteristic of carbonaceous materials at around 1580 cm^{-1}. Inserted images correspond to the sample within the diamond anvil cell chamber during the experiment.